Turbulence measurements in the Garonne river tidal bore: first observations

B. Simon[1,2], P. Lubin[1], D. Reungoat[1] and H. Chanson[2]
[1] Université de Bordeaux, I2M
16 avenue Pey-Berland, Pessac, France, CNRS UMR 5295, 33607 Pessac
FRANCE
[2] The University of Queensland, School of Civil Engineering
Brisbane St Lucia, QLD 4072
AUSTRALIA
E-mail: h.chanson@uq.edu.au

Abstract: *A tidal bore is an abrupt rise in water depth advancing in some estuaries during spring tide conditions. In the present study, some detailed turbulence field measurements were conducted continuously at high-frequency (64 Hz) in the Garonne River tidal bore. The turbulent velocity components were sampled with an acoustic Doppler velocimeter (ADV) at 0.8 m beneath the free-surface. On 10 and 11 Sept. 2010, the tidal bore was undular as it passed in front of the sampling site. The tidal bore Froude number estimated from the channel bathymetry and observations was equal to 1.20 and 1.30 on 10 and 11 Sept. 2010 respectively. The turbulent velocity data showed the marked impact of the tidal bore propagation. The longitudinal velocity component highlighted some rapid flow deceleration during the passage of the tidal bore, associated with a sudden rise in the free surface elevation, and a flow reversal after the tidal bore front passage. The Reynolds stress data indicated some large amplitudes and rapid fluctuations during the tidal bore and flood flow. These field observations are the first detailed turbulence measurements in a tidal bore with high spatial and temporal resolutions.*

Keywords: *Tidal bore, Garonne River, Field measurements, Unsteady turbulence, Acoustic Doppler velocimetry.*

1. INTRODUCTION

A tidal bore is a series of waves propagating upstream as the tidal flow turns to rising. It forms during spring tide conditions when the tidal range exceeds 4 to 6 m and the flood tide is confined to a narrow funnelled estuary. With time, the leading edge of the flood tidal wave becomes steeper and steeper until it forms a wall of water: i.e., the tidal bore (Bazin 1865, Chanson 2011). After the formation of the bore, there is an abrupt rise in water depth at the bore front that is discontinuity in the water depth, and pressure and velocity fields (Lighthill 1978). Figure 1 shows the tidal bore of the Garonne River in France.

To date, the turbulence field observations in tidal bores are very limited, often conducted with a very-coarse resolution in terms of temporal and spatial scales. In the present study, some detailed turbulence measurements were conducted continuously at high-frequency (64 Hz) prior to, during and after the tidal bore of the Garonne River in September 2010. The results provided an unique characterisation of the turbulence at 0.8 m beneath the free-surface during two tidal bore events.

2. FIELD INVESTIGATION AND INSTRUMENTATION

The field study was conducted in the Garonne River (France) in the Arcins channel between Arcins Island and the right bank close to Lastrene township. The Arcins channel (44°47'58"N, 0°31'07"W) is about 1.8 km long, 70 m wide and about 1.1 to 2.5 m deep at low tide (Fig. 1 & 2). Figure 2 presents a cross-sectional survey conducted on 10 Sept. 2010, with the location of the ADV sampling volume immediately prior to the tidal bore. Although the tides were semi-diurnal, the tidal cycles had slightly different periods and amplitudes indicating some diurnal inequality. The field measurements were conducted under spring tidal conditions on 10 and 11 September 2010. The tidal range in Bordeaux was 6.03 and 5.89 m respectively (Table 1). During the study, the water elevations and some

continuous high-frequency turbulence data were recorded prior to, during and after the passage of the tidal bore for a couple of hours on each day. Further information was reported in Chanson et al. (2010).

The free surface elevations were measured manually using a survey staff. During the passage of the tidal bore, a video camera recorded the water level and the data were collected frame by frame at 25 fps. The survey staff was mounted 1 m beside the ADV unit towards the right bank. The turbulent velocities were measured with a Nortek^{TM} Vector ADV (6 MHz, serial number VEC3332) sampled continuously at 64 Hz. The ADV system was equipped with a 3D downlooking head (Head ID VEC4665). The system was fixed at the downstream end of a 23.55 m long heavy, sturdy pontoon, mounted vertically with the positive direction head towards downstream. The ADV unit was mounted vertically between the pontoon hulls and the sampling volume was about 0.8 m below the free-surface. All the ADV data underwent a thorough post-processing procedure to eliminate any erroneous or corrupted data. The post processing included the removal of communication errors, the removal of average signal to noise ratio data less than 15 dB and the removal of average correlation values less than 60%. In addition, the phase-space thresholding technique developed by Goring and Nikora (2002) was applied to remove spurious points.

(A) Looking downstream at the incoming bore with Arcins Island on the left and the right bank on the right

(B) Undular tidal bore passing the ADV sampling location (Bottom right) - Pierre Lubin held the survey staff used to record the water depth (bottom right corner)

Fig. 1 - Tidal bore of the Garonne River at Arcins on 10 September 2010

Table 1 - Tidal bore properties in the Arcins channel (Garonne River, France) at the sampling location during the field experiments in September 2010

Date	Tidal range (m)	V_1 (m/s)	U (m/s)	A_1 (m^2)	B_1 (m)	A_1/B_1 (m)	Fr_1	Remarks
10/10/2010	6.03	+0.33	4.5	106	75.4	1.40	1.30	Undular bore.
11/09/2010	5.89	+0.30	4.2	109	75.8	1.43	1.20	Undular bore.

Notes: A_1: channel cross-section area immediately prior to the bore passage; B_1: free-surface width immediately prior to the bore passage; Fr_1: tidal bore Froude number; U: tidal bore celerity positive upstream on the channel centreline; V_1: downstream surface velocity on the channel centreline immediately prior to the bore passage.

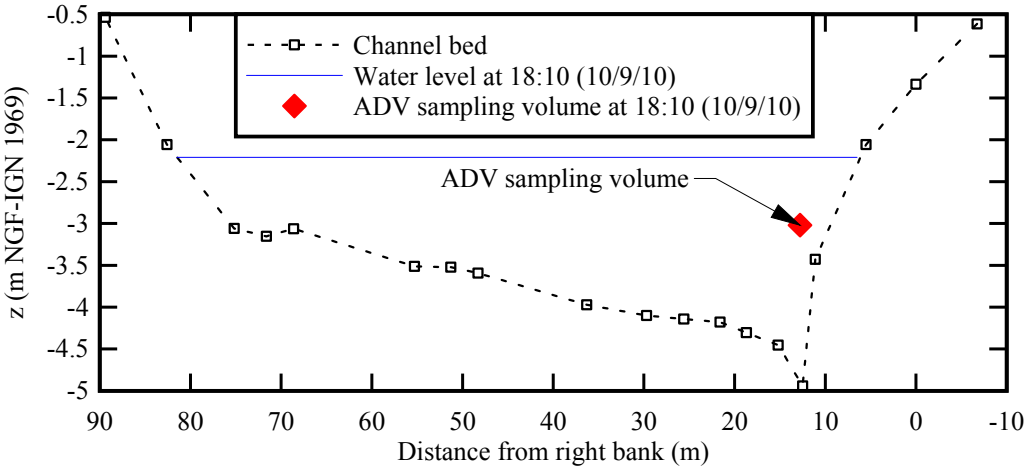

Fig. 2 - Surveyed cross-section of Arcins channel with the low tide water level on 10 Sept. 2010 afternoon and the corresponding ADV sampling volume and free-surface elevations prior to the tidal bore - Looking downstream

3. GENERAL OBSERVATIONS

The tidal bore propagation in the Arcins channel was observed on 10 and 11 Sept. 2010, and the flow patterns were similar on each day. The tidal bore formed first at the downstream end of the channel about 4 min 45 s before it reached the sampling location. Immediately after onset, the tidal bore expanded rapidly across the entire channel width as a breaking bore. As the bore propagated upstream, its shape evolved in response to the local bathymmetry. About 200 m downstream of the sampling point, the bore became undular and its front was flatter (Fig. 1). The tidal bore was undular as it passed in front of the sampling location, and some basic tidal bore characteristics are summarised in Table 1. The bore continued to propagate up to the upstream end of the Arcins channel for another 4 minutes in the form of an undular bore.

At the sampling location, the passage of the tidal bore was followed by a pseudo-chaotic wave motion lasting for several minutes after the bore. The free-surface elevation rose very rapidly by 0.50 m and 0.41 m in the first 5 seconds on 10 and 11 Sept. 2010 respectively. For the next 35 minutes, the water elevation rose further by 1.69 m and 1.59 m on 10 and 11 Sept. 2010 respectively.

In a tidal bore, the Froude number Fr_1 is always greater than unity. For $Fr_1 < 1$, the tidal wave cannot become a tidal bore (Lighthill 1978, Liggett 1994). For $1 < Fr_1 < 1.5$ to 1.8, the tidal bore is undular, and a breaking bore is observed for $Fr_1 > 1.5$ to 1.8. In an irregular channel, the tidal bore Froude number must account for the cross-sectional irregularity, and some momentum considerations yield:

$$Fr_1 = \frac{V_1 + U}{\sqrt{g \times \frac{A_1}{B_1}}} \quad (1)$$

where V_1 is the initial flow velocity positive downstream, U is the tidal celerity positive upstream, A_1 is the initial flow cross-section and B_1 is the initial free-surface width (Henderson 1966, Chanson 2004). The ratio A_1/B_1 represents an equivalent cross-sectional averaged water depth. During the present field experiments, the tidal Froude number was estimated from the surveyed channel cross-section, water level observations and tidal bore celerity observations (Table 1). Equation (1) yielded Fr_1 = 1.30 and 1.20 for the field observations on 10 and 11 Sept. 2010 respectively. The results were consistent with the observations of an undular tidal bore at the sampling location (Fig. 1).

The water depth was recorded about 1 m beside the ADV towards the right bank. The data were collected visually, but using a video camera (25 fps) during the bore passage. Figure 3 presents the 60 s period around the tidal bore front passage. The water depth data showed consistently the same trends, both qualitatively and quantitatively, on each day. The water depth decreased slowly during the end of the ebb tide prior to the tidal bore arrival (i.e. 0.20 m in 30 min). The passage of the bore was associated with a very rapid rise of the water elevation (Fig. 3) and some pseudo-chaotic wave motion shortly after. A frequency analysis showed no dominant wave frequency, but a superposition of a range of wave periods. During the following flood flow, the water depth increased rapidly with time: i.e., nearly 3 m in 90 minutes.

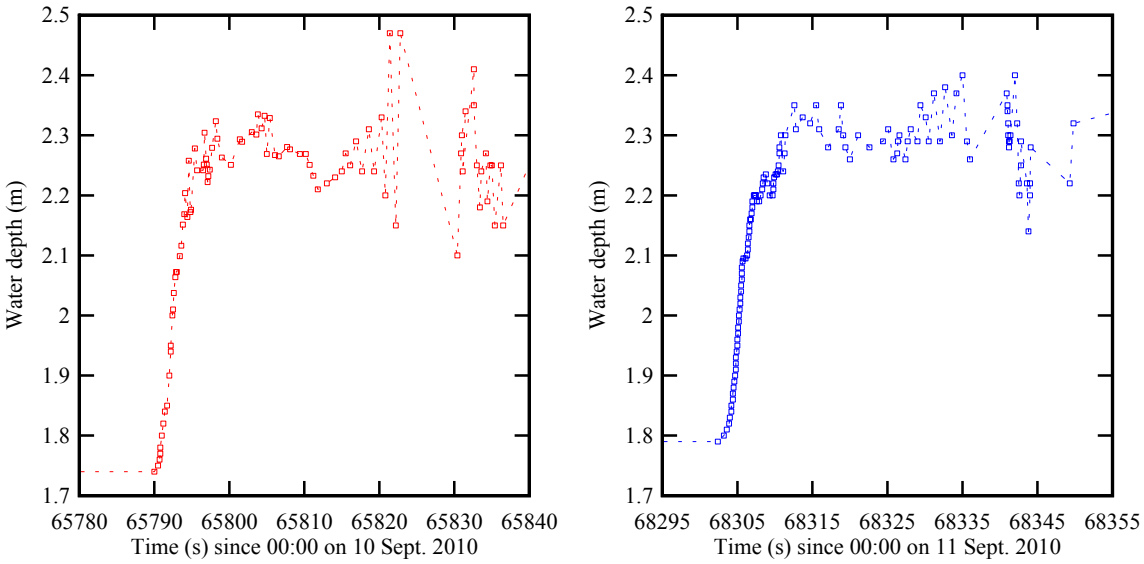

(A) On 10 Sept. 2010 (B) On 11 Sept. 2010

Fig. 3 - Time variations of the water depth during the field experiments

4. TURBULENT VELOCITY MEASUREMENTS

The turbulent velocity data highlighted a marked impact of the tidal bore (Fig. 4). Figure 4A shows the water depth and longitudinal velocity component V_x on 11 Sept. 2010 for a 50-s period around the bore passage, and Figure 4B presents the transverse and vertical velocity components, V_y and V_z respectively, where the longitudinal velocity component V_x is positive downstream, the transverse velocity component V_y is positive towards the Arcins Island (towards the left, Fig. 1A), and the vertical velocity component V_z is positive upwards.

The data showed the drastic impact of the passage of the bore front on the velocity at 0.8 m beneath the free-surface (Fig. 4A). The longitudinal velocity data highlighted some rapid flow deceleration during the passage of the bore front associated with a reversal in flow direction. As the bore front reached the sampling volume, the rise in free surface elevation was associated with a flow reversal seen in Figure 4A. The observations were consistent with the earlier observations of Wolanski et al. (2004) and Simpson et al. (2004) in the field, and Hornung et al. (1995), Koch and Chanson (2009) and Chanson (2010) in laboratory channels.

Visual observations indicated that the surface current was stronger in the channel centreline than close to the right bank, but the authors noted at times some recirculation patterns next the waterline

mark on the right bank where the surface velocity flowed at times downstream against the main flood flow direction.

The tidal bore passage was further characterised by some large fluctuations of all turbulent velocity components (Fig. 4). Both very rapid fluctuations and longer period oscillations were observed. The longitudinal flow component changed from +0.3 m/s (oriented downriver) to -1 m/s (oriented upriver) immediately after the passage of the bore, with turbulent fluctuations between -0.3 to -1.5 m/s behind the bore (Fig. 4A). This period of large velocity fluctuations lasted for the entire sampling duration (over 1 hour). The longitudinal velocity results were consistent with the free-surface observations before and after the tidal bore passage, although the water elevation and velocity were sampled at different rates, preventing a detailed phase-averaging analysis.

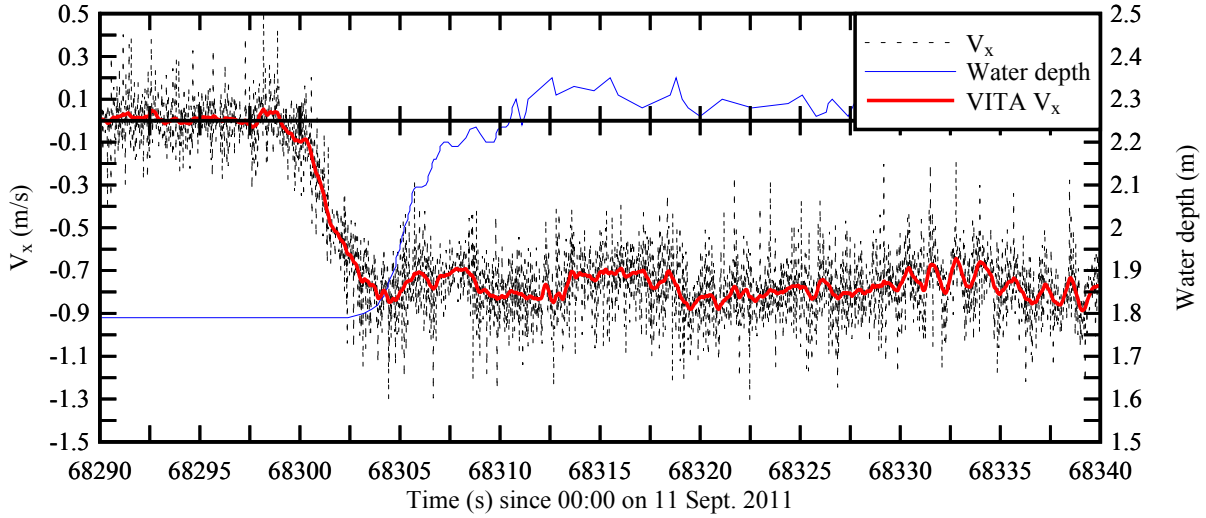

(A) Water depth and horizontal velocity component V_x (Instantaneous data and VITA)

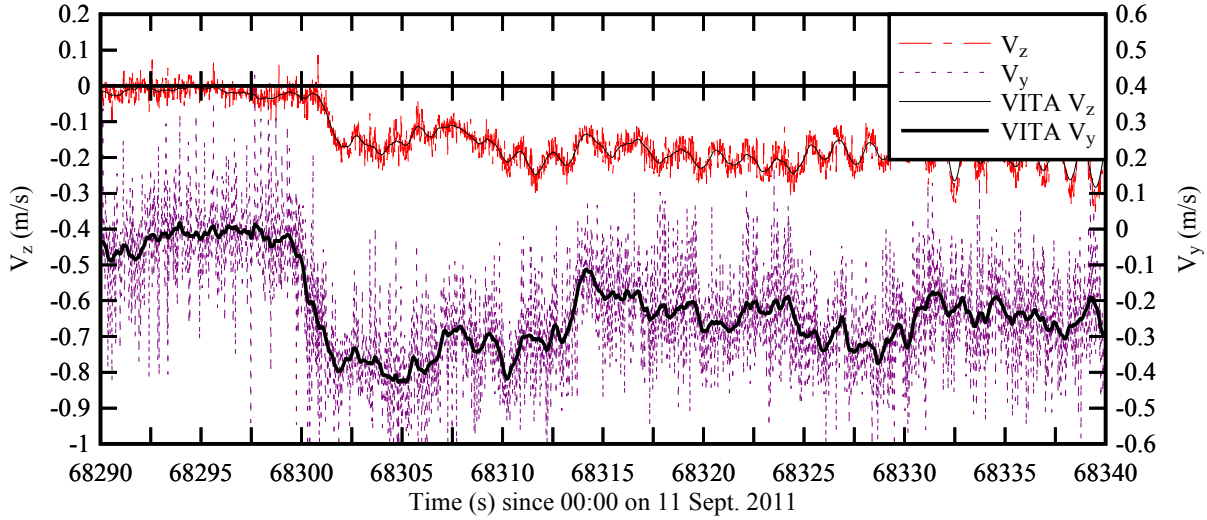

(B) Transverse and vertical velocity components (V_y, V_z) (Instantaneous data and VITA)

Fig. 4 - Water depth and turbulent velocity components during the tidal bore passage on 11 Sept. 2010 - Post-processed ADV data, sampling rate: 64 Hz

After the passage of the bore, the transverse velocity data fluctuated between 0 and -1.1 m/s, and the time-averaged transverse velocity component was -0.28 m/s (Fig. 4B). The finding implied some transverse circulation towards the right bank, at 0.8 m below the surface. The pattern was linked possibly with the existence of some secondary flow motion in the irregular channel cross-section, and the recirculation patterns observed next to the right bank. The vertical velocity data highlighted a marked effect of the tidal bore. After the bore passage, the vertical velocity fluctuated between +0.1 and -0.8 m/s, with a time-averaged value of about -0.28 m/s. Since the ADV sampling volume was located close to the free-surface, the vertical velocity fluctuations were constrained by the free-surface deformation rate. Note in Figure 4B that the vertical velocity data presented some quasi-periodic

fluctuations with periods of about 1.2 s about 400 s after the bore passage (t ~ 68,320 to 68,340 s). These were believed to be linked with some free-surface waves with a similar period that were visually observed (but not recorded with sufficient temporal resolution). Both Figures 4A and 4B include the instantaneous velocity data and the variable interval time averaged (VITA) velocity components. Both graphs have the same vertical and horizontal scales. A data analysis suggested that all the velocity fluctuations v' where 30 to 50% larger during the bore passage than those observed during the ebb tide prior to the bore, where v' is the standard deviation of the turbulent fluctuation around the VITA (figures not shown). Further the data implied $v_x' \approx v_y' > v_z'$; the smaller vertical velocity fluctuations remained unexplained, although this might be linked with the proximity of the free-surface which constrained the vertical velocity fluctuations.

During the study, the ADV sampling volume depth ranged from 0.7 to 0.9 m for the entire study duration. The velocity data characterised therefore the turbulent velocity field in the upper water column.

5. TURBULENT REYNOLDS STRESSES

The turbulent Reynolds stresses were calculated using a VITA method, following Koch and Chanson (2009) and Docherty and Chanson (2010), and shown in Figure 4. The signal was filtered using a band pass filter set between zero and a cutoff frequency deduced from a sensitivity analysis: F_{cutoff} = 1 Hz. The filtering was applied to all velocity components, and the turbulent Reynolds stresses were calculated from the high-pass filtered velocity components.

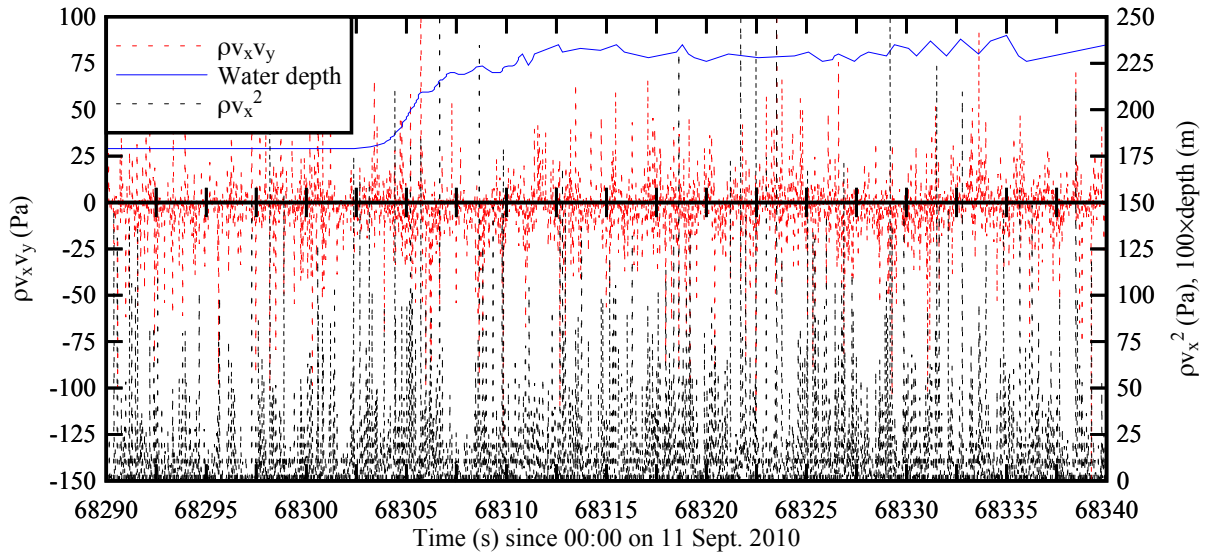

Fig. 5 - Time-variations of the Reynolds stresses $\rho \times v_x^2$ and $\rho \times v_x \times v_y$, and water depth during the tidal bore passage on 11 Sept. 2010 - Post-processed ADV data, sampling rate: 64 Hz

The Reynolds stress data showed some large and rapid turbulent stress fluctuations during the tidal bore and flood flow. The Reynolds stress magnitudes were generally larger than during the ebb tide, and some substantial normal and tangential stress fluctuations were observed. For example, in Figure 5, the normal stress $\rho \times \overline{v_x^2}$ was three times larger during the tidal bore than during the ebb flow prior to the bore. Figure 5 presents some results in terms of the Reynolds stresses $\rho \times v_x^2$ and $\rho \times v_x \times v_y$, using the same horizontal time scale as in Figure 4. The turbulent stress data illustrated the large amplitude and rapid fluctuations during and after the tidal bore (Fig. 5). Overall the Reynolds stress amplitudes were large with normal stress magnitudes up to 400 Pa and tangential stress magnitudes up to 250 Pa.

Despite some differences in geometry and flow conditions, a comparison in terms of turbulent stresses between field and laboratory data is pertinent for some comparable Froude number. The geometric scaling ratio between the present field study and the experiments of Koch and Chanson (2009) was 17.5:1. For an undistorted Froude similitude, the shear stress scaling ratio equals the geometric

scaling ratio, 17:5:1 herein (Liggett 1994, Chanson 2004). Any deviation would imply some scale effects in terms of the Reynolds stresses. The present shear stress magnitudes were typically 100 to 200 times larger than the laboratory data, suggesting some limitations of the Froude similarity, although no systematic study was conducted to date to assess the scale effects affecting the turbulent mixing in tidal bore flows.

6. CONCLUSION

Some detailed turbulence field measurements were conducted continuously at high-frequency (64 Hz) prior to, during and after the tidal bore of the Garonne River in September 2010. The field site was located in the Arcins channel close to the city of Bordeaux (France). The turbulent velocity components were sampled continuously with an acoustic Doppler velocimeter (ADV) whose sampling volume was located 0.8 m beneath the free-surface.

The tidal bore propagation in the Arcins channel was observed on 10 and 11 Sept. 2010. The bore was undular as it passed the sampling site. The tidal bore Froude number was estimated from the channel bathymetry and tidal bore observations. It was equal to 1.20 and 1.30 on 10 and 11 Sept. 2010 respectively, corresponding to an undular bore. The passage of the tidal bore was characterised by a pseudo-chaotic wave motion lasting for several minutes after the bore. At the sampling location, the free-surface elevation rose very rapidly with time: i.e., 0.4-0.5 m in the first 5 seconds and nearly 3 m during the next 90 minutes. The turbulent velocity data showed the marked impact of the tidal bore propagation. The longitudinal velocity component highlighted some flow deceleration during the passage of the tidal bore, associated with a rapid rise in the free surface elevation, and a flow reversal behind the tidal bore front. The tidal bore passage was further characterised by some large fluctuations of all three turbulent velocity components. The observations were consistent with some earlier field and laboratory results.

A striking feature of the present field data set was the large and rapid fluctuations in turbulent velocities and turbulent stresses during the tidal bore and flood flow. This was not documented to date, but an important difference between the ADV data set used herein from earlier reported field measurements was that the present data were collected continuously at relatively high frequency (64 Hz) during a relatively long period (at least 2 hours). However the present investigation was a point measurement at 0.8 m beneath the free-surface and any extrapolation to the entire channel cross-section would be inappropriate.

7. ACKNOWLEDGMENTS

The authors thank all the people who participated to the field works. They acknowledge the assistance of Patrice and the permission to access and use the pontoon in the Bras d'Arcins. The ADV was provided kindly by Dr Dominique Mouaze (University of Caen, France). They acknowledge the assistance of Dr Frederic Murzyn (ESTACA-Laval, France). Hubert Chanson acknowledges some financial assistance from the Université de Bordeaux and the University of Queensland; Bruno Simon acknowledges a joint scholarship funded by the TREFLE Laboratory and the Région Aquitaine; the financial assistance of the Agence Nationale de la Recherche (Projet Mascaret 10-BLAN-0911-01) is acknowledged.

8. REFERENCES

Bazin, H. (1865). *Recherches Expérimentales sur la Propagation des Ondes*. ('Experimental Research on Wave Propagation.') Mémoires présentés par divers savants à l'Académie des Sciences, Paris, France, Vol. 19, pp. 495-644 (in French).

Chanson, H. (2004). *The Hydraulics of Open Channel Flow: An Introduction*. Butterworth-Heinemann, Oxford, UK, 2nd edition, 630 pages.

Chanson, H. (2010). *Unsteady Turbulence in Tidal Bores: Effects of Bed Roughness*. Journal of Waterway, Port, Coastal, and Ocean Engineering, ASCE, Vol. 136, No. 5, pp. 247-256 (DOI: 10.1061/(ASCE)WW.1943-5460.0000048).

Chanson, H. (2011). *Current Knowledge in Tidal bores and their Environmental, Ecological and Cultural Impacts*. Environmental Fluid Mechanics, Vol. 11, No. 1, pp. 77-98 (DOI: 10.1007/s10652-009-9160-5).

Chanson, H., Lubin, P., Simon, B., and Reungoat, D. (2010). *Turbulence and Sediment Processes in the Tidal Bore of the Garonne River: First Observations.* Hydraulic Model Report No. CH79/10, School of Civil Engineering, The University of Queensland, Brisbane, Australia.

Docherty, N.J., and Chanson, H. (2010). *Characterisation of Unsteady Turbulence in Breaking Tidal Bores including the Effects of Bed Roughness*. Hydraulic Model Report No. CH76/10, School of Civil Engineering, The University of Queensland, Brisbane, Australia.

Goring, D.G., and Nikora, V.I. (2002). *Despiking Acoustic Doppler Velocimeter Data*. Jl of Hyd. Engrg., ASCE, Vol. 128, No. 1, pp. 117-126. Discussion: Vol. 129, No. 6, pp. 484-489.

Henderson, F.M. (1966). *Open Channel Flow*. MacMillan Company, New York, USA.

Hornung, H.G., Willert, C., and Turner, S. (1995). *The Flow Field Downstream of a Hydraulic Jump*. Jl of Fluid Mech., Vol. 287, pp. 299-316.

Koch, C., and Chanson, H. (2009). *Turbulence Measurements in Positive Surges and Bores*. Journal of Hydraulic Research, IAHR, Vol. 47, No. 1, pp. 29-40 (DOI: 10.3826/jhr.2009.2954).

Liggett, J.A. (1994). *Fluid Mechanics*. McGraw-Hill, New York, USA.

Lighthill, J. (1978). *Waves in Fluids*. Cambridge University Press, Cambridge, UK, 504 pages.

Simpson, J.H., Fisher, N.R., and Wiles, P. (2004). *Reynolds Stress and TKE Production in an Estuary with a Tidal Bore*. Estuarine, Coastal and Shelf Science, Vol. 60, No. 4, pp. 619-627.

Wolanski, E., Moore, K., Spagnol, S., D'Adamo, N., and Pattieratchi, C. (2001). *Rapid, Human-Induced Siltation of the Macro-Tidal Ord River Estuary, Western Australia*. Estuarine, Coastal and Shelf Science, Vol. 53, pp. 717-732.

Wolanski, E., Williams, D., Spagnol, S., and Chanson, H. (2004). *Undular Tidal Bore Dynamics in the Daly Estuary, Northern Australia*. Estuarine, Coastal and Shelf Science, Vol. 60, No. 4, pp. 629-636.